Accepted Manuscript

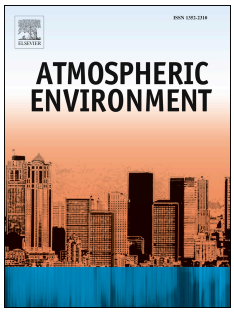

Diurnal, seasonal, and annual trends in tropospheric CO in Southwest London during 2000–2015: Wind sector analysis and comparisons with urban and remote sites

Iván Y. Hernández-Paniagua, David Lowry, Kevin C. Clemitshaw, Paul I. Palmer, Rebecca E. Fisher, James L. France, Alberto Mendoza, Simon O'Doherty, Grant Forster, M. Lanoisellé, Euan G. Nisbet

PII: S1352-2310(18)30041-4

DOI: 10.1016/j.atmosenv.2018.01.027

Reference: AEA 15786

To appear in: *Atmospheric Environment*

Received Date: 9 August 2017

Revised Date: 9 January 2018

Accepted Date: 13 January 2018

Please cite this article as: Hernández-Paniagua, Ivá.Y., Lowry, D., Clemitshaw, K.C., Palmer, P.I., Fisher, R.E., France, J.L., Mendoza, A., O'Doherty, S., Forster, G., Lanoisellé, M., Nisbet, E.G., Diurnal, seasonal, and annual trends in tropospheric CO in Southwest London during 2000–2015: Wind sector analysis and comparisons with urban and remote sites, *Atmospheric Environment* (2018), doi: 10.1016/j.atmosenv.2018.01.027.

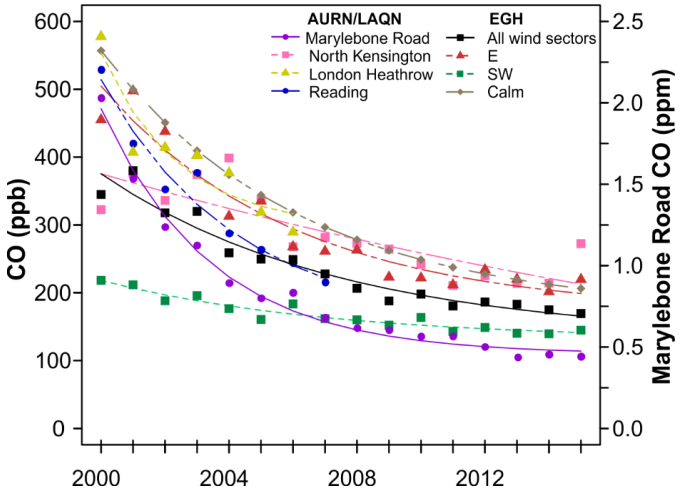

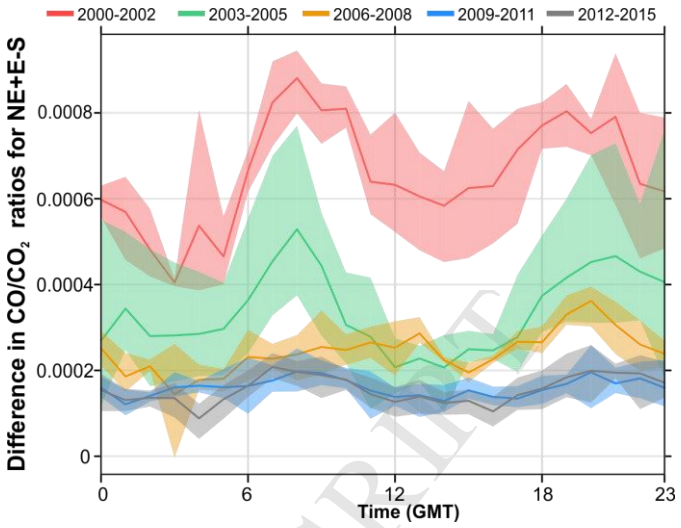

Diurnal, seasonal, and annual trends in tropospheric CO in Southwest London during 2000-2015: Wind sector analysis and comparisons with urban and remote sites

Iván Y. Hernández-Paniagua[1,2], David Lowry[1], Kevin C. Clemitshaw[1], Paul I. Palmer[3], Rebecca E. Fisher[1], James L. France[1,4,5], Alberto Mendoza[6], Simon O'Doherty[7], Grant Forster[4,8], M. Lanoisellé[1] and Euan G. Nisbet[1]*

[1]Department of Earth Sciences, Royal Holloway, University of London, Egham, Surrey, TW20 0EX, United Kingdom.

[2]Centro de Ciencias de la Atmosfera, Universidad Nacional Autónoma de México, Circuito de la Investigación Científica S/N, Ciudad Universitaria, Coyoacán, 04510, Ciudad de México, México.

[3]School of GeoSciences, University of Edinburgh, Alexander Crum Brown Road, Edinburgh, EH9 3FF, United Kingdom.

[4]Centre for Ocean and Atmospheric Sciences, School of Environmental Sciences, University of East Anglia, Norwich, NR4 7TJ, United Kingdom.

[5]British Antarctic Survey, High Cross, Cambridge, UK, CB3 0ET.

[6]Escuela de Ingeniería y Ciencias, Tecnologico de Monterrey, Av. Eugenio Garza Sada 2501, Monterrey, Nuevo León, México, C.P. 64849.

[7]School of Chemistry, University of Bristol, Cantock's Close, Bristol, BS8 1TS, United Kingdom.

[8]National Centre for Atmospheric Science, School of Environmental Sciences, University of East Anglia, Norwich, NR4 7TJ, United Kingdom.

*Corresponding author: e.nisbet@es.rhul.ac.uk.

Highlights

1. CO data recorded at Egham (EGH) in Southwest London during 2000-2015 were analysed.
2. CO varies on time scales ranging from minutes to inter-annual and annual cycles.
3. CO declined at EGH more slowly than in Central London, but from a much lower starting point.
4. The largest decline rates were observed for the calm and Eastern wind sectors.
5. Assessment of CO/CO_2 residuals confirmed a clear decline in CO during periods of increased vehicle traffic from 2000 to 2015.

Abstract

Ambient carbon monoxide (CO) and meteorological parameters measured at the Egham (EGH) semi-rural site in SW London during 2000-2015 have permitted wind sector analysis

of diurnal and seasonal cycles, and interpretation of long-term trends. CO daily amplitudes are used as a proxy for anthropogenic emissions. At EGH, morning and evening peaks in CO arise from the dominant contribution of road transport sources. Smaller amplitudes are observed during weekends than weekdays due to lower combustion emissions, and for mornings compared to evenings due to the timing of the development and break-up of the nocturnal inversion layer or planetary boundary layer (PBL). A wavelet transform revealed that the dominant mode of CO variability is the annual cycle, with apparent winter maxima likely due to increased CO emissions from domestic heating with summer minima ascribed to enhanced dispersion and dilution during the annual maximum of PBL mixing heights.

Over the last two decades, both mitigation measures to reduce CO emissions and also a major switch to diesel cars, have accompanied a change at EGH from the dominance of local diurnal sources to a site measuring close to Atlantic background levels in summer months. CO observed in the S and SW wind sectors has declined by 4.7 and 5.9 ppb yr^{-1} respectively. The EGH CO record shows the highest levels in the early 2000s, with levels in E and calm winds comparable to those recorded at background stations in Greater London. However, since 2012, levels in S-SW sector have become more comparable with Mace Head background except during rush-hour periods. Marked declines in CO are observed during 2000-2008 for the NE, E, SE (London) and calm wind sectors, with the smallest declines observed for the S, SW and W (background) sectors. For the majority of wind sectors, the decline in CO is less noticeable since 2008, with an apparent stabilisation for NE, E and SE after 2009. The EGH CO data record exhibits a similar but slower exponential decay, but from a much lower starting concentration, than do CO data recorded at selected monitoring sites in urban areas in SE England. CO/CO_2 residuals determined using a 1 h window data in the diurnal cycle demonstrate a clear decline in CO from 2000 to 2015 during daily periods of increased vehicle traffic, which is consistent with a sustained reduction in CO emissions from the road transport sector.

Keywords

Combustion emission ratio, exponential decay, road transport, spectral analysis.

1. Introduction

CO is emitted into the troposphere primarily as a product of incomplete combustion processes, including burning of fossil fuels, bio-fuels, and agricultural biomass (Fortems-Cheiney et al., 2011; Worden et al., 2013). In the troposphere, CO is formed by the oxidation of volatile organic compounds (VOCs), and plays a central role in tropospheric chemistry via its reaction with the OH radical to form carbon dioxide (CO_2) (Waibel et al., 1999;

Bergamaschi et al., 2000; Jenkin and Clemitshaw, 2000). Reduction in global CO may indirectly affect the climate by changing the atmospheric life-time of CH_4, which is also oxidised via reaction with OH (IPCC, 2013). The global budget for CO is estimated between 2.2-2.5 PgC yr^{-1}, with around 65% of anthropogenic origin. Annual CO emissions are estimated between 500-750 Tg from large-scale biomass burning, between 500 and 650 Tg from fossil and domestic fuel burning, between 700-800 Tg from CH_4 oxidation and around 100 Tg from natural sources (Bergamasschi et al., 2000; Holloway et al., 2000; Duncan et al., 2007; IPCC, 2007; Lin et al., 2008).

CO has an average life-time in the troposphere of around 2 months, although it is seasonally dependent, and may range from 10-30 days in tropical regions during summer, to 90 days and almost 12 months in high northern latitudes (Novelli et al., 1998; Staudt et al., 2001; Zhang et al., 2011). The hemispheric imbalance of higher CO mixing ratios in the Northern Hemisphere (NH) results in spatial and temporal variations, which can be compounded by changes in combustion emissions, long-range transport and natural events such as wildfires. For example, data recorded at background and marine sites at mid-northern latitudes exhibit stronger seasonality (large seasonal amplitude values, AV_s) than at sites in the Southern Hemisphere (SH) (Derwent et al., 1998; Novelli et al., 1998). The highest concentrations of CO are observed typically close to combustion sources (Yurganov et al, 2010), and therefore CO can be used as a proxy for local and regional air pollution, fossil fuel and biomass burning (Edwards et al., 2006).

During the last century, the atmospheric burden of CO varied significantly between decades. For instance, industrialisation in western nations during 1950-1980 resulted in an average global growth rate of around ~1 % CO yr^{-1} (1-2 ppb CO yr^{-1}) due to increased fossil fuel combustion (Zander et al., 1989; Yurganov et al., 1999). Since the 1990s, the introduction of policies to control CO emissions from vehicular sources in Europe and North America have decreased ambient CO by between 10-50 % in urban areas (Kuebler et al., 2001; Bigi and Harrison, 2010; von Schneidemesser et al., 2010), while rural and semi-rural areas experienced reductions of 5-25 % (0.1-10 ppb CO yr^{-1}) (Simmonds et al., 1997; Lin et al., 2008; Worden et al., 2013; Kumar et al., 2013). By contrast, rapid economic development of Asian nations since the 1990s has greatly increased CO emissions, which compensate globally for emissions reduction in Europe and North America (Kumar et al., 2013).

CO emissions in England decreased by around 75 % during 1990-2014, driven mostly by changes in road transport (NAEI, 2016). The major benchmark was the requirement for new petrol cars to be fitted with three-way catalysts since 1989, and the switch in fuel from petrol

to diesel. Data recorded within the London Air Quality Network (LAQN) in Greater London show a marked decline in ambient CO, which confirms the inventory trends (LAQN, 2016). For instance, von Schneidemesser et al. (2010) reported a decline in CO at the LAQN Marylebone Road site during 1998-2008 of 12 % yr^{-1}, from 1.6 to 0.53 ppm CO. At the LAQN North Kensington site, Bigi and Harrison (2010) observed a smaller decline of around 3 % yr^{-1} in CO during 1996-2008. More recently, Lowry et al. (2016) reported a marked decline in CO levels during 1997-2014, for air masses arriving at the semi-rural Egham site (EGH) having passed over Greater London, which was ascribed to the adoption of stringent control emissions.

Nevertheless, road transport sources remain a major driver of diurnal variations of CO in the London area (NAEI, 2016). Worldwide, average CO diurnal cycles in urban areas typically show morning and evening peaks, with a delay of 1-3 h from the rush-period. For instance, within urban and sub-urban areas of Beijing (Xu et al., 2011), Mexico City (Stephens et al., 2008), Seoul (Nguyen et al., 2010) and London (Bigi and Harrison, 2010), the morning peak normally occurs around 08:00-09:00 local time. Ambient CO decreases typically by mid-day due to reduced emissions with less vehicles and better traffic flow, and dilution during the widening of the PBL mixing height (Shaw et al., 2007; DfT, 2017; Pal et al., 2017). Reduced fossil fuel combustion in the road transport sector during weekends leads to lower levels of CO than during weekdays (Stephens et al., 2008; Grant et al., 2010b; DfT, 2017). Seasonal changes in CO emissions from residential heating, energy-production and road transport, and in meteorology such as the PBL mixing height, wind direction and speed, modify the diurnal profiles of atmospheric gases from season-to-season (e.g. Helfter et al., 2011; Hernández-Paniagua et al., 2015).

Long-term trends in tropospheric CO have been studied extensively worldwide (Schultz et al., 2015). However, to date, few studies have addressed diurnal, seasonal and annual variations at a site with contributions from local and regional sources of CO. This study presents 16-years of continuous, high-precision measurements of CO made at the EGH site in SW London. In order to assess local and regional sources, CO levels in air masses that have travelled over Greater London are compared with background levels during westerly Atlantic winds. Daily and seasonal cycles, and long-term annual trends in CO at EGH are compared with those observed at selected sites within the UK Automatic Urban and Rural Network (AURN) and LAQN. Furthermore, CO data recorded during westerly winds are contrasted with those recorded at the Mace Head (MHD) observatory on the west coast of Ireland to estimate local rates of change as result of air quality control policies.

2. Experimental

2.1. Sampling location

High-precision and high-frequency in-situ measurements of tropospheric CO were made during 2000-2015 at the Greenhouse Gas Laboratory of the Department of Earth Sciences (ES) at the EGH campus of Royal Holloway University of London. The EGH site is situated in Surrey, UK (51° 25’ 36” N, 0° 33’ 40” W), some 32 km WSW of Central London (Fig. 1a), and approximately 8 km SW of London Heathrow Airport, 1.8 km W of the M25 motorway, and 1 km SW of the town of Egham (Fig. 1b). Around 2 km W of EGH lies Windsor Great Park, which is a mix of forested and agricultural land, and covers an area of some 30 km^2. The SW sector is mostly sub-urban, with houses scattered between predominant woodland, while the E sector is dominated by Greater London. Further details of the EGH site have been provided recently (Hernández-Paniagua et al., 2015; Lowry et al., 2016).

2.2. CO measurement methodology, instrumentation and calibration

CO was measured in air sampled approximately 15 m above ground level via an air inlet manifold 3 m above the roof of the ES building. This single length of ½-inch OD Synflex tubing enters the laboratory and is connected to a KNF-Neuberger pump which draws in air at a flow rate of 20 L min^{-1}. After the pump, the air inlet splits to feed a suite of measurement instruments. Until the end of 2008, CO measurements were made every 30-mins with a Trace Analytical Reduction Gas Detector (RGD-2) instrument, precise to ±2 ppb CO, using two 1/8" packed columns in series: a Unibeads 1S and a Molecular Sieve 5A, with zero air as the carrier gas. Working standards were calibrated twice per month using NOAA CMDL-filled and analysed cylinders of ambient air within the range 168-304 ppb CO (Lowry et al., 2016).

Since January 2008, the monitoring of CO was improved with the installation of a Peak Performer Analyser 1 (PP1) reduced compound photometer, with columns and carrier gas as for the RGD-2. Measurements were made every 5-mins with a stated precision better than ±1 ppb CO. A working standard was measured twice daily with twice monthly calibration checks using a suite of NOAA CMDL-filled and analysed cylinders of ambient air containing 186-300 ppb CO. The RGD-2 and PP1 instruments were run simultaneously during 2008 to inter-compare measurements, with data in very good agreement in the range 80-600 ppb CO, and a post-calibration offset of 0±5 ppb CO, a correlation gradient of 0.92, an intercept of 14.45 ppb CO, an r value of 0.98 and $p<0.001$. Since 2008, the PP1 has been the primary source of CO data. Further details can be found elsewhere (Lowry et al., 2016).

CO data capture varied between 78-99% of the annual maximum despite occasional instrument downtime. Figure 2 shows data capture for 30-min CO averages recorded during 2000-2015. CO daily averages were calculated from 30-min data; monthly averages from CO daily averages, with annual averages derived from CO monthly averages. Data capture for wind speed ranged from 67-99%, for wind direction 76-99% and for air temperature, 88-99% (Fig. 2). CO_2 data capture at EGH varied between 89 and 99% of maximum possible yearly measurements. A data capture threshold of 75% was used to consider data valid. Further details of the EGH CO_2 record can be found elsewhere (Hernández-Paniagua et al., 2015).

2.3. AURN, LAQN, Weybourne (WAO) and Mace Head (MHD) CO data sets

The AURN is the UK's largest automatic monitoring network with data used to assess compliance against Objectives of the UK and EU Ambient Air Quality Directives (Defra, 2017). Currently, 136 monitoring sites are operative and perform measurements of ambient NO and NO_2 (collectively NO_x), sulphur dioxide (SO_2), ozone (O_3), CO and particulate matter (PM_{10} and $PM_{2.5}$) across the UK (Defra, 2017). Quality assurance and quality control (QA/QC) processes for the AURN data are carried out independently by Ricardo Energy & Environment. Hourly AURN CO data, valid with a minimum data capture of 90%, were obtained from the AURN web site (Table 1) (http://uk-air.defra.gov.uk/data). Hourly LAQN CO data, valid with a minimum data capture of 75%, were downloaded from the LAQN web site (Table 1) (http://www.londonair.org.uk/london/asp/datadownload.asp) (LAQN, 2016).

The MHD research station is located on the west coast of Ireland (53°20’ N, 9°54’ W), which is ideal to monitor Atlantic background air masses. Further details of the MHD site are provided in Derwent et al. (2002) and Messager et al. (2008). The MHD CO dataset is maintained by the University of Bristol as part of the UK DECC Network and Advanced Global Atmospheric Gases Experiment (AGAGE), and was obtained from the web site of the World Data Centre for Greenhouse Gases (WDCGG) of the World Meteorological Organisation (WMO) (http://ds.data.jma.go.jp/gmd/wdcgg). It currently spans continuous measurements of CO made from March 1994 to September 2013.

The Weybourne Atmospheric Observatory (WAO) is a Global Atmospheric Watch (GAW) Regional station located on the North Norfolk Coast, UK (52º57’02’’N, 1º07’19’’E, 15 m asl) (Penkett et al., 1999). The station is funded by the National Centre for Atmospheric Science (NCAS) through the Atmospheric Measurement Facility (AMF). Since 2008, high-precision long-term measurements have been made of atmospheric CO. Further details of the

measurement technique are provided in Forster et al. (2012). The data set currently spans CO data from March 2008 to date and was obtained through institutional collaboration. Data from the WAO is also available from the Centre for Environmental Data Analysis (CEDA).

2.4. Meteorology at EGH and wind sector and seasonal analyses

The climate at EGH is maritime and mild, with significant month-to-month variations in wind direction and speed during the year (Figure 3) (Hernández-Paniagua et al., 2015; Lowry et al., 2016). SW winds are most common as depressions track across the UK, whereas E winds are frequent during anti-cyclonic conditions. Relatively clean air arrives at EGH from the SW and SSW. By contrast, E air masses trajectories pass over Greater London (8.17 million people; ONS, 2011) before arrival at EGH. During slow-moving anti-cyclonic air conditions in winter and early spring, the initial relatively clean air is augmented by combustion emissions from the London basin. Figure 3 shows that overall during 2000-2015, the predominant wind direction at EGH was SW, occurring between 17.9 and 24.7 % of the time in spring and winter, respectively. The largest frequency of high wind speeds is observed for winter and contrasts with the lowest frequency of calm events observed 11.5 % of the total time.

To perform wind-sector analyses, the EGH dataset was divided into 8 wind sectors of 45° starting from 0° ± 22.5° and an additional calm category (<0.1 m s^{-1}). The lower bound of each sector was established by adding 0.5° to avoid data duplicity. Seasons were defined according to temperature records in the NH: winter (December to February), spring (March to May), summer (June to August) and autumn (September to November).

2.6. Mathematical analyses

The CO data sets were analysed extensively with the *openair* package (Carslaw and Ropkins, 2012; Carslaw and Beevers, 2013) for R software (R Core Team, 2013). Long-term trends were computed as described previously (Hernández-Paniagua et al., 2015), with the MAKESENS 1.0 macro (Salmi et al., 2002) used to test the presence of a statistically significant monotonic linear trend. MAKESENS relies on the non-parametric Mann-Kendall test to estimate the slope and intercept of a linear trend, which is quantified with the non-parametric Sen's method. Long-term trends from the MAKESENS macro were compared with those obtained with the Theil-Sen tool included in the *openair* package. All results presented here did not show statistical differences (p>0.05) between both tests.

To identify and isolate seasonal features, the EGH CO dataset was spectrally decomposed using a wavelet transform that preserves frequency variations as a function of time, and

allows for the time evolution of signals (Torrence and Compo, 1998). This represents a major advantage over the Fourier transform, which implicitly assumes that a time series is stationary, e.g. the average and variance do not change with time. Typically, the wavelet transform (and the Fourier transform) assumes equally spaced data in time or space, although adapted transform methods can address unevenly spaced data. In the case of time series of atmospheric CO, the wavelet transform can identify changes in the phase and amplitude of CO that may result from changes in the timing and magnitude of emissions. The wavelet transform has been previously applied to Arctic CO_2 (Barlow et al., 2015), CO (Mackie et al., 2016), and CH_4 (Barlow et al., 2016).

Seasonal cycles, secular trends and residual components were computed using the seasonal-trend decomposition technique (STL) developed by Cleveland et al. (1990) as described previously (Hernandez-Paniagua et al., 2015). Statistical analyses were performed with the computational software SPSS 19.0 for Microsoft Windows.

3. Results and discussion

3.1 Time-series in CO recorded at EGH during 2000-2015

The EGH CO dataset exhibits recurrent seasonal cycles and pollution episodes, and a clear sustained decline in the maximum observed values from 2000 to 2008 (Fig. 4). High CO mixing ratios, >1000 ppb, were frequently recorded before 2008, mostly during winter, with lowest values recorded during summer. Table 2 provides annual descriptive statistics for the entire dataset. By the early 2000s, the CO levels (> 400 ppb) recorded in E and calm winds arriving at EGH are similar to those recorded at North Kensington and Marylebone Rd in Central London (Bigi and Harrison, 2010; von Schneidemesser et al., 2010). By contrast, the annual average CO levels observed for the S-SW sectors at EGH since 2012 are not far above the overall averages measured at MHD (Lowry et al., 2016). In addition to this pronounced decline, winter-time pollution episodes have also decreased in severity. Satellite measurements of decreasing tropospheric CO over Europe agree with the apparent decline of CO observed in EGH, which is also observed above North America (Yurganov et al., 2010; Fortems-Cheiney et al., 2011; Pommier et al., 2013; Worden et al., 2013; Lowry et al., 2016).

3.2 Daily and weekly cycles of CO at EGH

Diurnal variations in CO arise from changes in emissions from combustion sources and meteorology, mostly in the PBL mixing height (Grant et al., 2010b; Hossain et al., 2012; Defra, 2017). Figure 5 shows normalised daily cycles for CO at EGH, derived from hourly averages, by season and day of the week during 2000-2015. During weekdays, positive

correlations between the increases in CO and traffic flow for Greater London were observed during morning (r=0.93) and evening (r=0.87), while over weekends, only morning increases exhibited a significant correlation (r=0.97) (DfT, 2017). These correlations suggest a dominant contribution of road transport sources to the CO daily cycle as discussed by Bigi and Harrison (2010). Monitoring sites that experience air masses with relatively minor combustion sources typically exhibit a single CO peak in the daily cycle (An et al., 2013; Lee et al., 2015). The trough in the CO daily cycles observed in all seasons arise from combination of a dilution effect due to the growth of the PBL mixing height that is independent of day of the week (Pal et al., 2017), and reductions in CO emissions from lower traffic flow during the maximum mixing height of the PBL (Bohnenstengel et al., 2015).

Trough-to-peak amplitude values of the CO diurnal cycles (AV_d) were calculated for morning and evening peaks for weekends and weekdays to assess diurnal variations in ambient CO. At EGH, morning AV_d values are lower than evening values for all seasons, with Sunday values being the lowest of the week. This is in good agreement with traffic data for Greater London that shows the greatest traffic volume typically occurring during weekdays between 16:00-18:00 GMT (DfT, 2017). For all days, the largest CO AV_d are observed in winter and the lowest in summer driven by the PBL mixing height (Lee et al., 2015). This is in good agreement with the maximum PBL mixing heights in Central London of around 2000 m during summer, some 7-10 h after sunrise, and <1500 m during winter, some 5-7 h after sunrise (Xie et al., 2013; Halios and Barlow, 2017), which appears to be coupled with the seasonal timing of the CO daily cycle trough, although no significant correlation (p>0.05) was observed. The longer persistence of the evening CO peak for all seasons can be attributed to the stability of the PBL height overnight that affects the dispersion of evening CO emissions, which is clearly observed during winter (Grant et al., 2010b).

3.3 CO annual cycles at EGH

A wavelet transform was used to spectrally decompose the EGH CO data set to describe periodic variations with time. The mathematical discussion of this approach and further details of the parameters used can be found elsewhere (Barlow et al., 2015). Figure 6 shows the power spectrum of the CO data. The original CO time series can be reconstructed with an accuracy of much less than 1% from the spectrally decomposed information determined by the wavelet transform. The region below the cone of influence (Fig. 6a) is the boundary below which wavelet coefficients are most compromised by edge effects. As might be anticipated from inspection of the raw data, the dominant mode of CO variability is the

annual cycle (Fig. 6b), and the annual and sub-annual periods dampen with time in response to a gradual reduction in peak mixing ratios (Mackie et al., 2016).

While the global power spectrum is strongly peaked at one year, the power is spread across neighbouring periods, reflecting the temporal resolution of the data. Consequently, periods of between 10 and 15 months are conservatively used to study the annual cycle. The peak at a month is explained by anomalous large values during 2000-2001 (Fig. 4). Changes in periodicity between diurnal and annual cycles are likely due to staged emission reductions, as discussed in Section 3.5 (NAEI, 2016). Using the wavelet transform as a band-pass filter a subset of periods can be isolated, for example, by retaining periods > 15 months, the seasonal cycle is effectively removed from the data. The resulting annual growth rate initially shows substantial year-to-year variation, but generally has a downward trend that tapers off after 2008. The annual cycle (periods of 10-15 months) behaves like a damped oscillator (with the exception of 2007/2008) that shows progressively smaller amplitudes with time. The sub-annual cycle (periods < 10 months) shows large year-to-year variations, even after the large drop from 2000 to 2004 (Fig. 4), although there does appear to be a general tendency to get smaller with time.

To determine typical maxima and minima occurrence in CO at EGH, de-trended average annual CO cycles by wind sector were obtained by subtracting annual averages from each monthly average, which removes the impact of long-term trends (Fig. 7). The average annual CO cycles at EGH exhibit apparent winter maxima and summer minima, in agreement with other studies in the NH (Simmonds et al., 1997; Derwent et al., 1998; Novelli et al., 1998; Bigi and Harrison, 2010). No significant variations (p>0.05) were observed in the averages of daily traffic volume in Greater London, which could lead to fairly constant CO vehicular emissions throughout the year (DfT, 2017). However, increased CO emissions from domestic heating together with a decreased PBL mixing height may contribute to the elevated mixing ratios observed during winter for all wind sectors (Xie et al., 2013; NAEI, 2016; Halios and Barlow, 2017).

The occurrence of frequent E and NE air masses at EGH that potentially transport CO emitted from Greater London under low PBL mixing height conditions are likely to cause the largest peak observed in the CO cycle during winter for those wind sectors. However, the calm wind sector (wind speeds <0.1 m s^{-1}) exhibits the largest annual variability (Fig. 4), with a peak between December-January arising from the accumulation of local combustion sources during periods characterised by stable atmospheric conditions and temperature inversions. This can be confirmed by the lowest CO mixing ratios observed for the

background S and SW sectors, which suggests a low contribution from other CO sources during winter. By contrast, the lowest CO mixing ratios are observed during summer for all wind sectors, with the largest amplitude detected for calm and the lowest for the background sector. During summer, enhanced convective conditions promote dispersion of CO emissions leading to troughs in the annual cycle. This is supported by the diagnosed PBL mixing heights at the London Heathrow site made by Xie et al. (2013) for clear days of summer (June) and winter (November) of 2007, who reported that overall the daytime PBL mixing height on a calm winter day is much lower at 500 m, compared to 1700 m for summer. This is in good agreement with the average PBL mixing heights estimated for summer and winter by Bohnenstengel et al. (2015) based on a turbulence threshold at two sites in SE England, where deeper mixing heights during summer than during winter arise from enhanced convective forcing from surface sensible heat fluxes.

3.4 Wind sector analysis of long-term trends in CO at EGH

The secular trends of CO at EGH by wind sector during 2000-2015 were calculated from annual averages, derived from monthly averages filtered with the STL technique (Cleveland et al., 1990). The best fitting for the whole EGH CO data record is given by an offset exponential function as reported by Lowry et al. (2016). Figure 8 shows exponential fittings for all wind sectors at EGH and the parameterisation of the trends. Overall, marked declines in CO are observed during 2000-2008 for the NE, E, SE and calm, with the lowest declines observed for the S, SW and W wind sectors. For the majority of wind sectors, the decline in CO is less noticeable since 2008, with an apparent stabilisation for NE, E and SE after 2009. When the trends in CO are linearised with the Mann-Kendall approach, the declines for all wind sectors are significant at $p<0.001$ as listed in Table 3. The linear declines range from 4.7 ppb CO yr^{-1} (2.4 % yr^{-1}) to 18.7 ppb CO yr^{-1} (4.8 % yr^{-1}) for S and E wind sectors, respectively. As in the exponential fitting, the largest declines correspond to the NE, E, SE and calm winds sectors, with decreases in CO of 60.8-76.8 % during 2000-2015.

The decline rates in CO of 4.7 and 5.9 ppb CO yr^{-1} observed for the S and SW wind sectors at EGH (Table 3) are consistent with the 2.65 ± 0.04 ppb CO yr^{-1} recorded during 1991-2004 at Jungfraujoch, Switzerland (Zellweger et al., 2009), but considerably greater than the 0.84 ± 0.95 ppb CO yr^{-1} recorded at Zugspitz, Germany during 1991-2004 (Chevalier et al., 2008). At EGH, CO levels in SW and S air masses are close to Atlantic CO values because of relatively few significant CO emissions sources over SW England. This explains the lowest decline rates in CO observed for such wind sectors, and is ascribed to the abatement of more minor CO emission sources than those observed for the urban sectors. By contrast, the large declines in CO for the NE, E and calm wind sectors (the London sectors) are

significantly lower than that at North Kensington of ca. 50 ppb CO yr^{-1} during 1996-2008 (Bigi and Harrison, 2010), and represent around 15 to 20 % of that of ca. 98 ppb yr^{-1} at Marylebone Rd during 1998-2008 (von Schneidemesser et al., 2010). Kuebler et al. (2001) reported larger CO decline rates for urban sites than for rural sites over Switzerland, which is in agreement with the decline rates observed for the different wind sectors at EGH. This is consistent with the rapid abatement of large CO sources such as road transport, followed by a slower reduction in the remaining sources (Lowry et al., 2016; NAEI, 2016).

3.5 Decline of CO in the London area and comparison with the UK NAEI

EGH trends are compared with those estimated for representative long-term sites within Greater London to put the decline in CO estimated at EGH in the context of SE England. Figure 9 shows the comparison of trends in CO for LAQN sites over Greater London and the urban centre Reading (REA) (around 30 km NW of EGH), with representative EGH wind sectors during 2000-2015. Note the difference in scale for MY1. The LAQN/AURN CO trends follow an exponential decay and can be represented by the exponential function proposed for EGH by Lowry et al. (2016) with fittings ranging from R^2 = 0.74 for KC1 to R^2 = 0.96 for REA (Supplementary Information, Table S1). Parameterisation of the trends from 2000 to 2015 indicates the largest decline occurred at MY1 (78 %, i.e. 4.9 % yr^{-1}) with the smallest decline at LH2 (16 %, i.e. 1.0 % yr^{-1}). Annual declines in CO at MY1 and KC1 of ca. 12 % yr^{-1} and 3 % yr^{-1} during 1998-2008 and 1996-2008, respectively (von Schneidemesser et al. (2010); Bigi and Harrison, 2010), are around 2.5-3 times greater than those determined here for such sites from 2000 to 2015. The differences in CO declines arise from assessment of different time periods, and are consistent with effective abatement of large CO sources during the late 1990s and early 2000s, as evidenced by the large declines observed for LH2 and REA during 2000-2007.

The CO declines for the LAQN/AURN sites assessed during 2000-2015 agree with those observed for the EGH NE, E and calm wind sectors but differ significantly from the EGH S and SW wind sectors. The UK NAEI reports an overall decline in CO emissions of 59 % from 2000 to 2014. This decline followed two major changes in the vehicle fleet. The first was legislation in the 1990s for more rigorous control on exhaust emissions from petrol-fuelled vehicles, coupled with tax switches to make leaded petrol more expensive than unleaded (hence reducing poisoning of exhaust catalysts by leaded fuel) (Lowry et al., 2016). Secondly, there has been a sharp increase in diesel vehicles that reached about 50% of sales in 2016 (DfT, 2016), which has reduced CO emissions but increased pollution from emissions of NO_x (Beevers et al., 2016).

Figure 10a shows that the largest reduction in CO emissions is for road transport, which is estimated at around 84 % (5.6 % yr^{-1}) during 2000-2014 (NAEI, 2016), and is similar to that reported here for MY1 kerbside site during 2000-2015. Although, CO emissions from the road transport sector still remain significant, currently, the largest reported source is stationary combustion. Figure 10b shows that CO recorded at EGH for E and calm wind sectors decrease in a similar way as NAEI CO emissions estimates. The increase in CO observed in 2010 is likely due to cold weather experienced during winter as reported by the UK NAEI (2016), which triggered CO stationary combustion emissions from the residential sector. It is also possible that a 4-fold increase in the use of biomass for industrial combustion since 2008 may have offset reductions in emissions from other sources (NAEI, 2016).

3.6 Mace Head and WAO comparison

Figure 11 compares normalised CO daily cycles at EGH and MHD during 2000-2013, calculated from hourly averages relative to the daily average. Larger peak-to-trough amplitudes are evident at EGH than at MHD, especially during 2000-2008. The largest apparent decline in CO amplitudes at EGH is observed for the morning peak and E wind sector. By 2013, the daily cycles for SW EGH wind sector are close to those observed at MHD, although a morning peak at EGH is still apparent. The larger amplitudes in CO at EGH arise from emission of significant CO sources in SE England, which are absent at MHD. Both, the morning and evening CO peaks coincide with the traffic rush hours, which suggests a large contribution of road transport sources not detected at MHD (An et al., 2013).

Figure 12 shows the comparison among the long-term trends in CO at EGH for E, SW, calm and all wind sectors from 2000 to 2015 calculated from de-seasonalised annual averages with those estimated at MHD during 2000-2013 for the whole data set and at WAO for SW and all wind sectors during 2009-2015. CO at MHD shows a significant (p<0.05) increasing linear trend of 0.84 ppb CO yr^{-1} in marked contrast with the exponential declines for CO recorded at EGH. At WAO, the whole CO data set shows an increase of 0.29 ppb yr^{-1} in contrast with a decrease for the SW of 0.34 ppb yr^{-1}, although both are not significant (p>0.05). The increasing trend at MHD and for the SW at WAO are opposite to that observed at the Pico Mountain Observatory (PMO) in the Azores of -0.31 ppb yr^{-1} during 2001-2011 (Kumar et al., 2013), which was ascribed to decrease in CO anthropogenic emissions from North America. Grant et al. (2010a) reported that during the occurrence European polluted air masses at MHD, background levels of hydrogen increase on average 5.3 ppb, likely due to the transport of primary emissions from fossil fuel combustion. Such

continental transport could explain the increases in CO observed at MHD and WAO, which is not observed at the PMO because of the small influence from European air masses.

The decrease in CO observed for the SW wind sector at WAO is in good agreement with those seen at EGH and can be explained by the reduction in road transport emissions reported in the UK NAEI (2016) for SE England. Hence, during cyclonic conditions air mass trajectories may travel from EGH to WAO, entraining emissions from the Greater London. After 2013, CO at EGH, WAO and MHD are comparable during SW air masses. However, at EGH the E and calm wind sectors exceed MHD and WAO values by around 80 and 50 ppb, respectively, despite significantly reduced CO emissions in SE England, and particularly London, since 2000 (NAEI, 2016).

3.7 CO/CO_2 ratio

The ratio of CO/CO_2 provides further insight into changes in combustion emissions of CO as it is not affected by dilution processes due to boundary layer dynamics (Chandra et al., 2016). To assess the decrease in road transport emissions of CO, the CO/CO_2 residual was defined as the excess CO/CO_2 in air from the NE and E wind sectors compared with the S wind sector: i.e. the residual value when the hourly averaged CO/CO_2 ratio for the S wind sector is subtracted from CO/CO_2 ratios for the NE and E wind sectors. During anti-cyclonic conditions, NE and E air masses may transport combustion emissions from Greater London to EGH, while during cyclonic conditions, EGH encounters background Atlantic air.

Figure 13 shows diurnal variations of CO/CO_2 residuals during 2000-2015 using a 1 h data averaging window in the diurnal cycle for 4 periods of 3-yr, and for 2012-2015. The CO/CO_2 residuals demonstrate a clear decline in CO from 2000 to 2015 during periods of increased vehicle traffic, with the largest declines during 2000-2008. Table S2 lists cumulative declines in CO/CO_2 daily residuals. Overall, during the whole period, declines of 72 and 75 % are observed for the maxima and average CO/CO_2 daily residuals, respectively, although a decline of 91 % is observed for the minima CO/CO_2 daily residuals. These declines are consistent with the sustained reduction in CO emissions from the road transport sector, and with the early abatement of larger CO sources followed by a more difficult reduction in remaining sources (NAEI, 2016).

4. Conclusions

Long-term trends for CO data recorded at EGH from 2000 to 2015 are addressed using a wind sector analysis, traffic and emissions data, as well as comparison with urban and

remote monitoring sites. CO varies on time scales ranging from hourly to daily at EGH, with seasonal and inter-annual cycles. CO 1-h mixing ratios recorded during 2000-2008 have declined clearly in magnitude, simultaneously with the occurrence of severe episodes. Since 2010, the largest 1-h CO mixing ratios measured are similar to the lowest ones observed in the early 2000s. Diurnal cycles in CO are driven by the PBL height and changes in road transport emissions. CO seasonal cycles arise from changes in meteorological conditions and emissions, with winter maxima coincident with the greatest emissions from stationary combustion and minima occurring under conditions of enhanced convection. Continuous monitoring of the PBL mixing height at or near the EGH site would aid interpretation of the CO dynamics observed, especially as access to such data recorded nearby at Heathrow is restricted. This would also help to inform future policy directives focused on air pollution abatement strategies through better understanding of the influence of meteorological processes on air pollutants.

The wind sector analysis carried out revealed that the largest CO mixing ratios are measured in air masses from the E and NE, which arrive at EGH after passing over Greater London and Heathrow airport. By contrast, the lowest CO mixing ratios are recorded for air masses from the S and SW wind sectors. The long-term trend in CO at EGH follows an exponential decay, with the largest rate of change observed during 2001-2008, and for the NE, E and calm wind sectors. Linearised trends in CO from 2000 to 2015 suggest declines of 4.7 and 18.7 ppb yr^{-1} for S and E wind sectors, respectively. The declines in CO for the urban wind sectors follow the exponential decrease observed for monitoring sites in Greater London, although the latter declines more rapidly.

When compared with CO recorded at MHD, the EGH CO mixing ratios are significantly higher with larger daily amplitudes in response to road transport emissions. From 2000 to 2013, MHD and WAO exhibit an increasing long-term trend, which contrasts with the exponential decline in CO at EGH. However, the SW sector at WAO does exhibit a non-significant decreasing trend comparable to that for the SW sector at EGH. The decline in CO recorded at EGH during 2000-2015 comes from the significant decrease in CO emissions, and is consistent with the reduction in emissions from the road transport sector following introduction in the late 1990s of stricter controls by UK and EU legislation to improve air quality, and also, paradoxically, the dieselisation of the car fleet, that otherwise greatly increased pollution. The S-SW sector is now comparable with MHD background except during rush-hour periods. London has a long record of CO pollution (Evelyn, 1772): the progress made with CO in the past two decades demonstrates the feasibility of bringing all pollutants down to near-background levels.

5. Acknowledgements

Grant-aided support to I.Y. Hernández-Paniagua from the Mexican National Council of Science and Technology (CONACYT, scholarship number 215094) and Public Education Ministry (SEP) is gratefully acknowledged. The RHUL Greenhouse Gas Laboratory has been supported by NERC, HEFCE, the EU and RHUL since 1994. P.I.P. gratefully acknowledges support from his Royal Society Wolfson Research Merit Award. The operation of the Mace Head atmospheric station was supported the Department of Business Energy and Industrial Strategy (BEIS, UK) (contract GA0201 to the University of Bristol).

6. References

An, X., Sun, Z., Lin, W., Jin, M., Li, N. (2013). Emission inventory evaluation using observations of regional atmospheric background stations of China. J. Environ. Sci-China, 25(3), 537-546.

Barlow, J.M., Palmer, P.I., Bruhwiler, L.M., Tans, P. (2015). Analysis of CO_2 mole fraction data: first evidence of large-scale changes in CO_2 uptake at high northern latitudes. Atmos. Chem. Phys., 15, 13,739-13,758.

Barlow, J.M., Palmer, P.I., Bruhwiler, L.M. (2016). Increasing boreal wetland emissions inferred from reductions in atmospheric CH_4 seasonal cycle, Atmos. Chem. Phys. Discuss., 752, 2016.

Beevers, S., Carslaw, C., Dajnak, D., Stewart, G., Williams, M., Fusell, J., Kelly, F. (2016). Traffic management strategies for emissions reduction: recent experience in London. Energy Emiss. Control Technol. 4, 27-39.

Bergamaschi, P., Hein, R., Heimann, M., Crutzen, P.J. (2000). Inverse modeling of the global CO cycle 1. Inversion of CO mixing ratios. J. Geophys. Res., 105(D2), 1909-1927.

Bigi, A., Harrison, R.M. (2010). Analysis of the air pollution climate at a central urban background site. Atmos. Env., 44(16), 2004-2012.

Bohnenstengel, S.I., Belcher, S. E., Aiken, A., Allan, J.D., Allen, G., Bacak, A., et al. (2015). Meteorology, air quality, and health in London: The ClearfLo project. Bull. Amer. Meteor. Soc, 96(5), 779-804.

Carslaw, D.C., Ropkins, K. (2012). openair - An R package for air quality data analysis. Environ. Modell. Soft., 27-28, 52-61.

Carslaw, D.C., Beevers, S.D. (2013). Characterising and understanding emission sources using bivariate polar plots and k-means clustering. Environ. Modell. Soft., 40, 325-329.

Carslaw, D.C. (2015). The openair manual - open-source tools for analysing air pollution data. Manual for version 1.0, King's College London.

Chandra, N., Lal, S., Venkataramani, S., Patra, P. K., Sheel, V. (2016). Temporal variations of atmospheric CO_2 and CO at Ahmedabad in western India. Atmos. Chem. Phys., 16(10), 6153-6173.

Chevalier, A., Gheusi, F., Attié, J.L., Delmas, R., Zbinden, R., Athier, G., Counsin, J.M. (2008). Carbon monoxide observations from ground stations in France and Europe and long-term trends in the free troposphere. Atmos. Chem. Phys. Discuss., 8, 3313-3356.

Cleveland, R.B., Cleveland, W.S., McRae, J., Terpenning, I. (1990). STL: a seasonal-trend decomposition procedure based on loess. J. Off. Stats., 6(1), 3-33.

Defra, 2017. Pollutant Information: Carbon Monoxide**.** National Atmospheric Emissions Inventory. Available at: http://naei.defra.gov.uk/overview/pollutants?pollutant_id=4. Last access: 1 Dec 2017.

Department for Transport (DfT). (2016). Vehicle Licensing Statistics: Quartes 4 (Oct - Dec) 2015. Available at: https://www.gov.uk/government/uploads/system/uploads/attachment_data/file/516429/vehicle-licensing-statistics-2015.pdf. Last access: 17 Dec 2017.

Department for Transport (DfT). (2017). Road Traffic Estimates: Great Britain 2016. Available at: https://www.gov.uk/government/collections/. Last access: 1 Dec 2017.

Derwent, R.G., Simmonds, P.G., Seuring, S., Dimmer, C. (1998). Observation and interpretation of the seasonal cycles in the surface concentrations of ozone and carbon monoxide at Mace Head, Ireland from 1990 to 1994. Atmos. Environ., 32(2), 145-157.

Derwent, R.G., Ryall, D.B., Manning, A., Simmonds, P.G., O'Doherty, S., Biraud, S. (2002). Continuous observations of carbon dioxide at Mace Head, Ireland from 1995 to 1999 and its net European ecosystem exchange. Atmos. Environ., 36(17), 2799-2807.

Duncan, B.N., Logan, J.A., Bey, I., Megretskaia, I.A., Yantosca, R.M., Novelli, P.C., Jones, N. B., Rinsland, C.P. (2007). Global budget of CO, 1988-1997: Source estimates and validation with a global model. J. Geophys. Res., 112(D22301).

Edwards, D.P., Emmons, L.K., Gille, J.C., Chu, A., Attié, J.L., Giglio, L., Wood, S.W., Haywood, J., Deeter, M.N., Massie, S.T., Ziskin, D.C., Drummond, J.R. (2006). Satellite-observed pollution from Southern Hemisphere biomass burning. J. Geophys. Res., 111(D14312).

Evelyn, J. (1772). Fumifugium or, the inconvenience of the aer, and smoake of London dissipated. Together with some remedies humbly proposed by JE Esq; to his sacred Majestie, and To the Parliament now Assembled. Published by His Majesties Command. W. Godbid for G. Bedel and T. Collins. 26pp. Available at: https://quod.lib.umich.edu/e/eebo/A38788.0001.001?c=eebo;c=eebo2;g=eebogroup;rgn=works;view=toc;xc=1;rgn1=author;q1=evelyn. Last access: 1 Aug 2017.

Forster, G.L., Sturges, W.T., Fleming, Z.L., Bandy, B.J., Emeis, S. (2012). A year of H_2 measurements at Weybourne Atmospheric Observatory, UK. Tellus Ser. B Chem. Phys. Meteorol., 64, 17771.

Fortems-Cheiney, A., Chevallier F., Pison I., Bousquet P., Szopa S., Deeter M. N., and Clerbaux C. (2011). Ten years of CO emissions as seen from Measurements of Pollution in the Troposphere (MOPITT). J. Geophys. Res. 116(D05304).

Grant, A., Witham, C.S., Simmonds, P.G., Manning, A.J., O'Doherty, S. (2010a). A 15 year record of high-frequency, in situ measurements of hydrogen at Mace Head, Ireland. Atmos. Chem. Phys., 10(3), 1203-1214.

Grant, A., Stanley, K.F., Henshaw, S.J., Shallcross, D.E., O'Doherty, S. (2010b). High-frequency urban measurements of molecular hydrogen and carbon monoxide in the United Kingdom. Atmos. Chem. Phys., 10(10), 4715-4724.

Halios, C.H., Barlow, J.F. (2017). Observations of the morning development of the urban boundary layer over London, UK, taken during the ACTUAL project. Boundary-Layer Meteorol., 1-28.

Helfter, C., Famulari, D., Phillips, G.J., Barlow, J.F., Wood, C.R., Grimmond, C.S.B., Nemitz, E. (2011). Controls of carbon dioxide concentrations and fluxes above central London. Atmos. Chem. Phys., 11(5), 1913-1928.

Hernández-Paniagua, I.Y., Lowry, D., Clemitshaw, K.C., Fisher, R.E., France, J.L., Lanoisellé, M., Ramonet, M., Nisbet, E.G. (2015). Diurnal, seasonal, and annual trends in atmospheric CO_2 in Southwest London during 2000-2012: Wind sector analysis and comparison with Mace Head, Ireland. Atmos. Environ., 105, 138-147.

Holloway, T., H. Levy II, Kasibhatla, P. (2000). Global distribution of carbon monoxide. J. Geophys. Res., 105(D10), 12,123-12,147.

Hossain, K.M.A., Easa, S.M. (2012). Pollutant dispersion characteristics in Dhaka City, Bangladesh. Asia-Pac. J. Atmos. Sci. 48(1), 35-41.

IPCC, 2007: Climate Change 2007: The Physical Science Basis. Contribution of Working Group I to the Fourth Assessment Report of the Intergovernmental Panel on Climate Change [Solomon, S., D. Qin, M. Manning, Z. Chen, M. Marquis, K.B. Averyt, M.Tignor and H.L. Miller (eds.)]. Cambridge University Press, Cambridge, United Kingdom and New York, NY, USA.

IPCC, 2013: Climate Change 2013: The Physical Science Basis. Contribution of Working Group I to the Fifth Assessment Report of the Intergovernmental Panel on Climate Change [Stocker, T.F., D. Qin, G.-K. Plattner, M. Tignor, S.K. Allen, J. Boschung, A. Nauels, Y. Xia, V. Bex and P.M. Midgley (eds.)]. Cambridge University Press, Cambridge, United Kingdom and New York, NY, USA, 1535 pp.

Jenkin, M.E., Clemitshaw, K.C. (2000). Ozone and secondary photochemical pollutants: Chemical processes governing their formation in the planetary boundary layer. Atmos. Environ., 34(16), 2499-2527.

Kuebler, J., Van Den Bergh, H., Russell, A.G. (2001). Long-term trends of primary and secondary pollutant concentrations in Switzerland and their response to emission controls and economic changes. Atmos. Environ., 35(8), 1351-1363.

Kumar, A., Wu, S., Weise, M.F., Honrath, R., Owen, R.C., Helmig, D., Kramer, L., Val Martin, M., Li, Q. (2013). Free-troposphere ozone and carbon monoxide over the North Atlantic for 2001-2011. Atmos. Chem. Phys., 13(24), 12,537-12,547.

Lee, T.R., De Wekker, S.F., Pal, S., Andrews, A.E., Kofler, J. (2015). Meteorological controls on the diurnal variability of carbon monoxide mixing ratio at a mountaintop monitoring site in the Appalachian Mountains. Tellus Ser. B Chem. Phys. Meteorol., 67(1), 25659.

Lin, Y.C., Lan, Y.Y., Tsuang, B.-J., Engling, G. (2008). Long-term spatial distributions and trends of ambient CO concentrations in the central Taiwan basin. Atmos. Environ., 42(18), 4320-4331.

London Air Quality Network (LAQN). (2017). Environmental Research Group, King's College London. Web site: http://www.londonair.org.uk/LondonAir/Default.aspx. Last access: 1 Dec 2017.

Lowry, D., Lanoiselle, M., Fisher, R.E., Martin, M., Fowler, C.M.R., France, J.L., Hernandez-Paniagua, I.Y., Novelli, P.C., Sriskantharajah, S., O'Brien, P., Rata, N.D., Holmes, C.W., Fleming, Z.L., Clemitshaw, K.C., Zazzeri, G., Pommier, M., McLinden, C.A., Nisbet, E.G.. (2016). Marked long-term decline in ambient CO mixing ratio in SE England, 1997-2014: Evidence of policy success in improving air quality. Sci. Rep. 6, 25661.

Mackie, A.R., Palmer, P.I., Barlow, J.M., Finch, D.P., Novelli, P., Jaeglé, L. (2016). Reduced Arctic air pollution due to decreasing European and North American emissions. J. Geophys. Res., 121(14), 8692-8700.

Messager, C., Schmidt, M., Ramonet, M., Bousquet, P., Simmonds, P., Manning, A. Ciais, P. (2008). Ten years of CO_2, CH_4, CO and N_2O fluxes over Western Europe inferred from atmospheric measurements at Mace Head, Ireland. Atmos. Chem. Phys. Discuss., 8(1), 1191-1237.

Nguyen, H., Kim, K., Ma, C., Cho, S., Sohn, J. (2010). A dramatic shift in CO and CH_4 levels at urban locations in Korea after the implementation of the natural gas vehicle supply (NGVS) program. Environ. Res., 110(4), 396-409.

Novelli, P.C., Masarie, K.A., Lang, P.M. (1998). Distributions and recent changes of carbon monoxide in the lower troposphere. J. Geophys. Res. D103(15), 19015-19033.

Office for National Statistics (ONS) – 2011 Census: Key Statistics and Quick Statistics for Local Authorities in the United Kingdom. (2013). Available at:

https://www.ons.gov.uk/employmentandlabourmarket/peopleinwork/employmentandemployeetypes/bulletins/keystatisticsandquickstatisticsforlocalauthoritiesintheunitedkingdom/2013-12-04. Last access: 21 Jun 2017.

Pal, S., Lee, T.R., De Wekker, S.F.J. (2017). A study of the combined impact of boundary layer height and near-surface meteorology to the CO diurnal cycle at a low mountaintop site using simultaneous lidar and in-situ observations. Atmos. Environ. 164, 165-179.

Penkett, S.A., Plane, J.M.C., Comes, F.J., Clemitshaw, K.C. (1999). The Weybourne Atmospheric Observatory. J. Atmos. Chem. 2(2), 107-110.

Pommier, M., Mclinden, C. A., Deeter, M. (2013). Relative changes in CO emissions over megacities based on observations from space. Geophys. Res. Lett., 40(14), 3766-3771.

R Core Team. (2013). R: a Language and Environment for Statistical Computing. R Foundation for Statistical Computing, Vienna, Austria, ISBN 3-900051-07-0.

Torrence, C. and Compo, G. P. (1998). A practical guide to wavelet analysis, B. Am. Meteorol. Soc., 79, 61-78.

von Schneidemesser, E., Monks, P.S., Plass-Duelmer, C. (2010). Global comparison of VOC and CO observations in urban areas. Atmos. Environ., 44(39), 5053-5064.

Salmi, T., Määttä, A., Anttila, P., Ruoho-Airola, T., Amnell, T. (2002). Detecting trends of annual values of atmospheric pollutants by the Mann-Kendall test and Sen's slope estimates – the Excel template application MAKESENS. Publications on Air Quality Report code FMI-AQ-31, (31)1-35. Helsinki, Finland.

Schultz, M.G., Akimoto, H., Bottenheim, J., Buchmann, B., Galbally, I.E., Gilge, S., Helmig, D., Koide, H., Lewis, A.C., Novelli, P.C., Plass-Dülmer, C., Ryerson, T.B., Steinbacher, M., Steinbrecher, R., Tarasova, O., Tørseth, K., Thouret, V., Zellweger, C. (2015). The Global Atmosphere Watch reactive gases measurement network. Elem. Sci. Anth., Oct 16(3).

Shaw, W.J., Pekour, M.S., Coulter, R.L., Martin, T.J., Walters, J.T. (2007). The daytime mixing layer observed by radiosonde, profiler, and lidar during MILAGRO. Atmos. Chem. Phys. Discuss., 7, 15025-15065.

Simmonds, P.G., Seuring, S., Nickless, G., Derwent, R.G. (1997). Segregation and interpretation of ozone and carbon monoxide measurements by air mass origin at the TOR Station Mace Head, Ireland from 1987 - 1995. J. Atmos. Chem., 28(1-3), 45-59.

Staudt, A. C., Jacob, D. J., Logan, J. A., Bachiochi, D., Krishnamurti, T. N., Sachse, G. W. (2001). Continental sources, transoceanic transport, and interhemispheric exchange of carbon monoxide over the Pacific. J. Geophys. Res. 106(D23), 32571-32589.

Stephens, S., Madronich, S., Wu, F., Olson, J. B., Ramos, R., Retama, A., Muñoz, R. (2008). Weekly patterns of México City's surface concentrations of CO, NO_x, PM_{10} and O_3 during 1986-2007. Atmos. Chem. Phys., 8(17), 5313-5325.

UK National Atmospheric Emissions Inventory (NAEI) (2016). Air quality pollutant inventories for England, Scotland, Wales and Northern Ireland: 1990 - 2014. A report of the National Atmospheric Emissions Inventory. Available at: http://naei.defra.gov.uk/. Last access: 1 Dec 2017.

Waibel, A.E., Fischer, H., Wienhold, F.G., Siegmund, P.C., Lee, B., Ström, J., Lelieveld, J., Crutzen, P.J. (1999). Highly elevated carbon monoxide concentrations in the upper troposphere and lowermost stratosphere at northern midlatitudes during the STREAM II summer campaign in 1994. Chemosphere Global Change Sci., 1(1-3), 233-248.

Worden, H.M., Deeter, M.N., Frankenberg, C., George, M., Nichitiu, F., Worden, J., Aben, I., Bowman, K.W., Clerbaux, C., Coheur, P.F., De Laat, A.T.J., Detweiler, R., Drummond, J.R., Edwards, D.P., Gille, J.C., Hurtmans, D., Luo, M., Martínez-Alonso, S., Massie, S., Pfister, G., Warner, J.X. (2013). Decadal record of satellite carbon monoxide observations. Atmos. Chem. Phys. 13(2), 837-850.

Xie, B., Hunt, J.C., Carruthers, D.J., Fung, J.C.H., Barlow, J.F. (2013). Structure of the planetary boundary layer over Southeast England: Modeling and measurements. J. Geophys. Res. 118(14), 7799-7818.

Xu, W.Y., Zhao, C.S., Ran, L., Deng, Z.Z., Liu, P.F., Ma, N., Lin, W.L., Xu, X.B., Yan, P., He, X., Yu, J., Liang, W.D., Chen, L.L. (2011). Characteristics of pollutants and their correlation to meteorological conditions at a suburban site in the North China Plain. Atmos. Chem. Phys., 11(9), 4353-4369.

Yurganov, L.N., Grechko, E.I., Dzhola, A.V. (1999). Zvenigorod carbon monoxide total column time series: 27-yr of measurements. Chemosphere Global Change Sci., 1(1-3), 127-136.

Yurganov, L., W. McMillan, E. Grechko, Dzhola, A. (2010). Analysis of global and regional CO burdens measured from space between 2000 and 2009 and validated by ground-based solar tracking spectrometers. Atmos. Chem. Phys. 10(8), 3479-3494.

Zander, R., Demoulin, P., Ehhalt, D.H., Schmidt, U., Rinsland, C.P. (1989). Secular increase of the total vertical column abundance of carbon monoxide above central Europe since 1950. J. Geophys. Res., 94(D8), 11,021-11,028.

Zellweger, C., Hüglin, C., Klausen, J., Steinbacher, M., Vollmer, M., Buchmann, B. (2009). Inter-comparison of four different carbon monoxide measurement techniques and evaluation of the long-term carbon monoxide time series of Jungfraujoch. Atmos. Chem. Phys., 9(11), 3491-3503.

Zhang, R., Wang, M., Ren, L. (2011). Long-term trends of carbon monoxide inferred using a two-dimensional model. Chemosphere Global Change Sci., 3(2), 123-132.

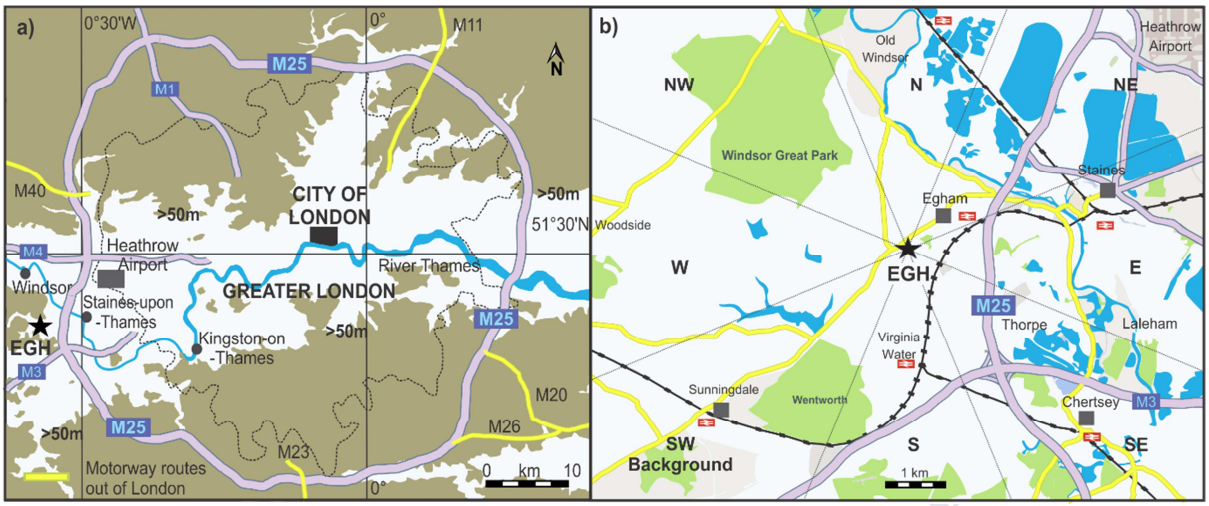

Fig. 1. a). Location of the EGH site and M25 motorway in relation to the Greater London area. b). EGH site and London motorway routes in the local context, and wind sectors definition. Adapted from: OpenStreetMap contributors (2015). Retrieved from https://planet.openstreetmap.org.

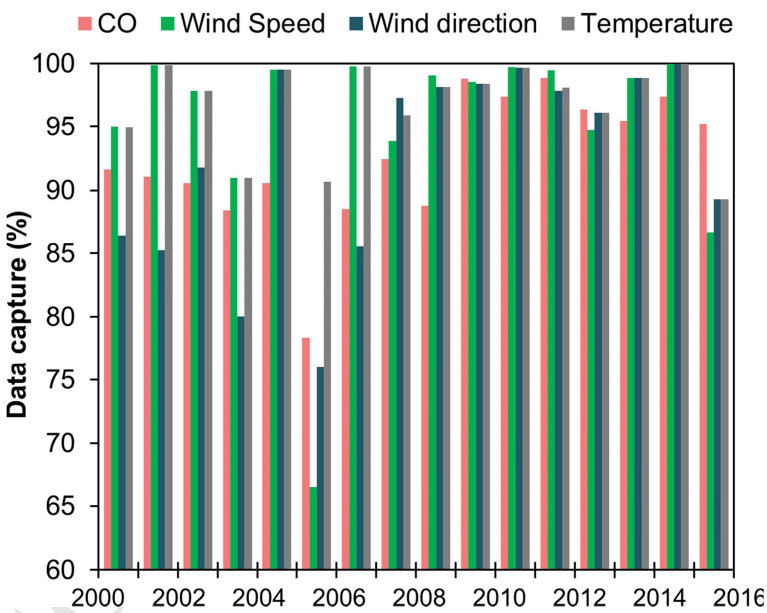

Fig. 2. Data capture of 30-min values for CO, wind speed, wind direction and temperature during 2000-2012 at EGH.

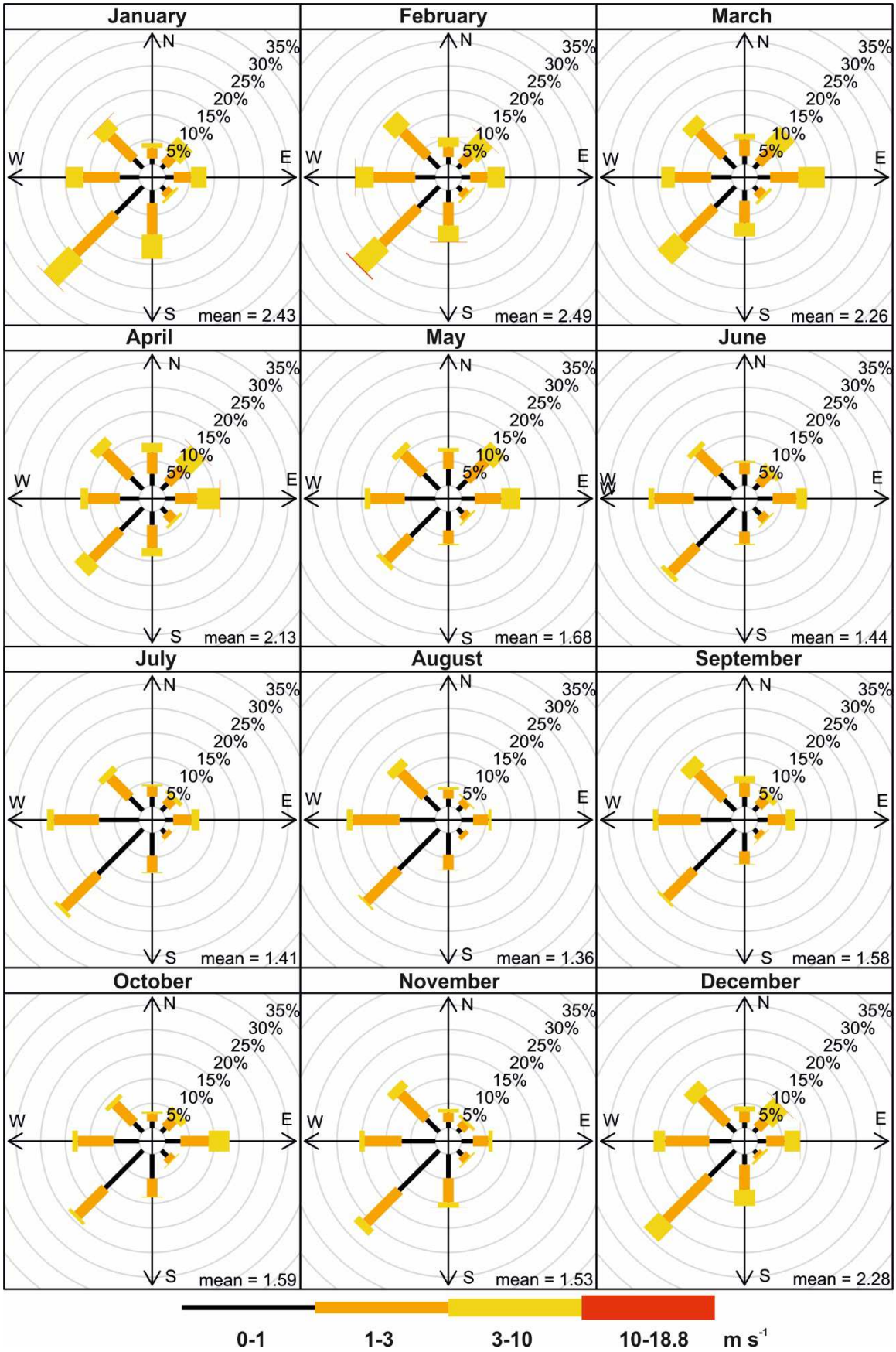

Fig. 3. Frequency of counts of measured wind direction occurrence by month at EGH during 2000-2015.

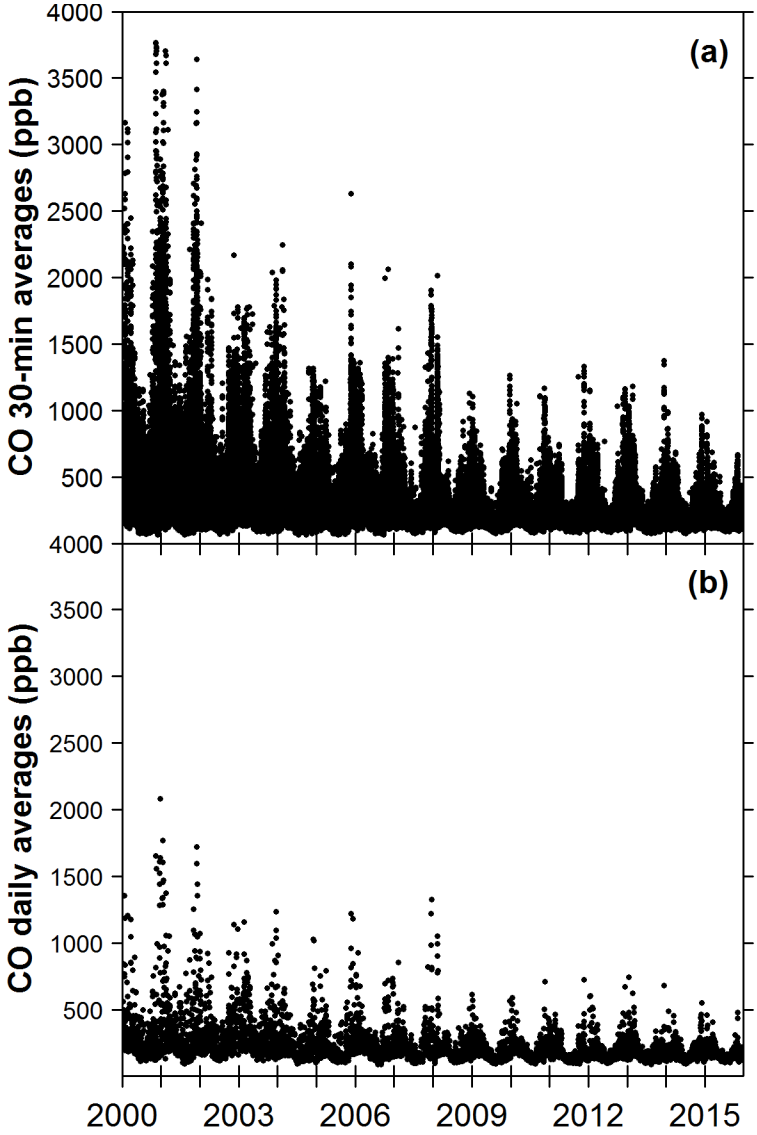

Fig. 4. a). 30-minute averages of CO during 2000-2012 at EGH. b). Daily averages during the same period.

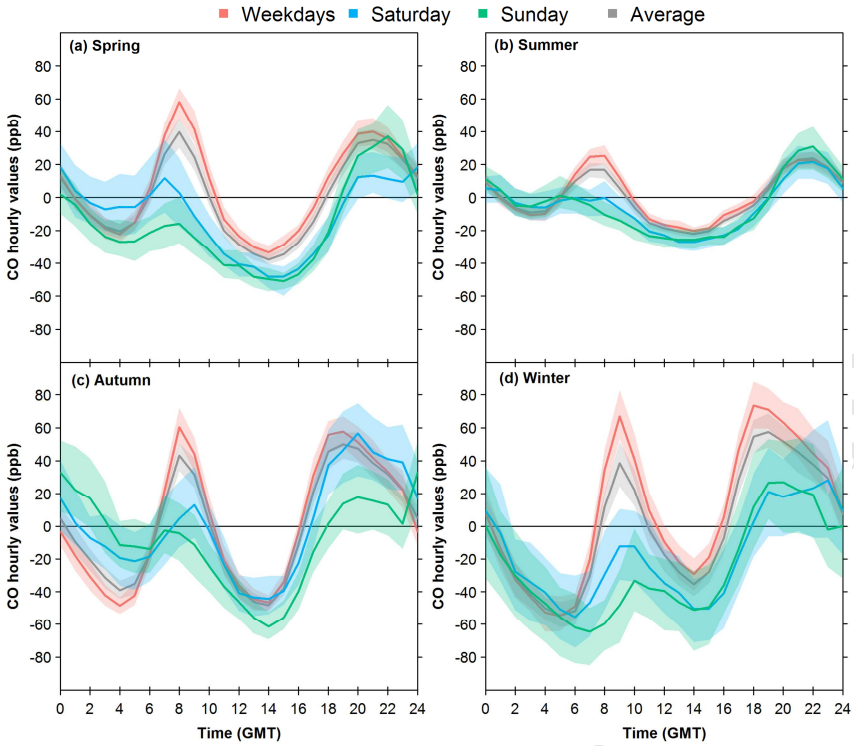

Fig. 5. CO normalised diurnal cycles by season at EGH during 2000-2015. The shadings show the 95 % confidence intervals of the averages calculated through bootstrap resampling (Carslaw, 2015).

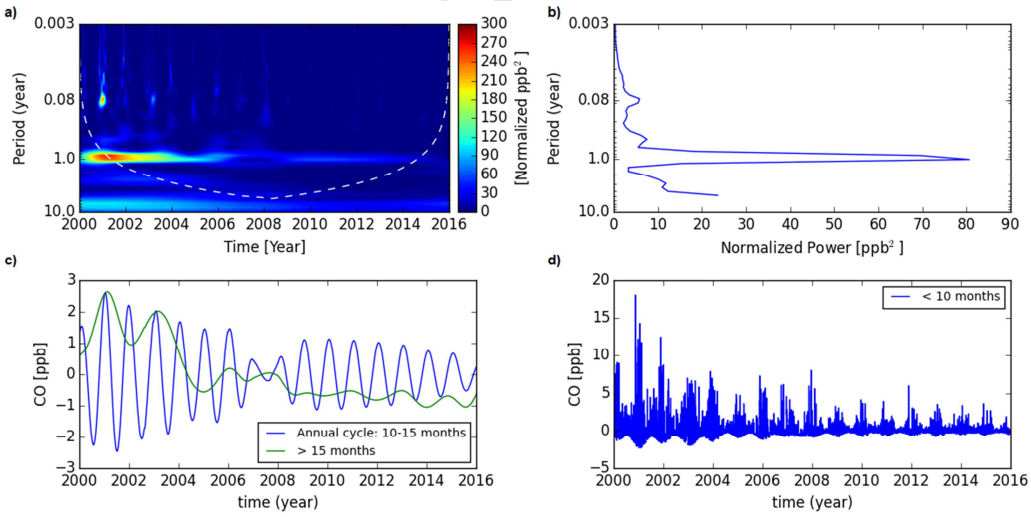

Fig. 6. Spectral de-composition of the CO data set recorded at EGH from 2000 to 2015. **a).** The wavelet power of the data, where warmer colours denote higher power. Values that sit below the cone of influence (white dashed line) are affected by edge effects and have a higher uncertainty and are not considered further, where 0.08 corresponds around to 1 month and 0.003 corresponds approximately to 1 day. **b).** The associated global wavelet spectrum, which represents a time integral of power. **c).** The seasonal (10-15 months), and low-variations (>15 months) and **d).** High-frequency variations (< 10 months) of CO as a function of time.

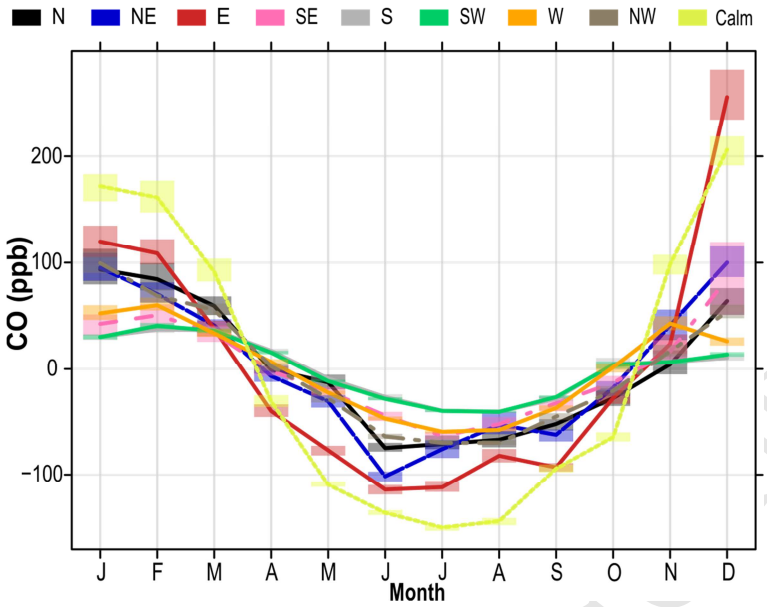

Fig. 7. De-trended average annual CO cycles by wind sector at EGH during 2000-2015. The shading shows the estimated 95 % confidence intervals estimated through bootstrap resampling (Carslaw, 2015).

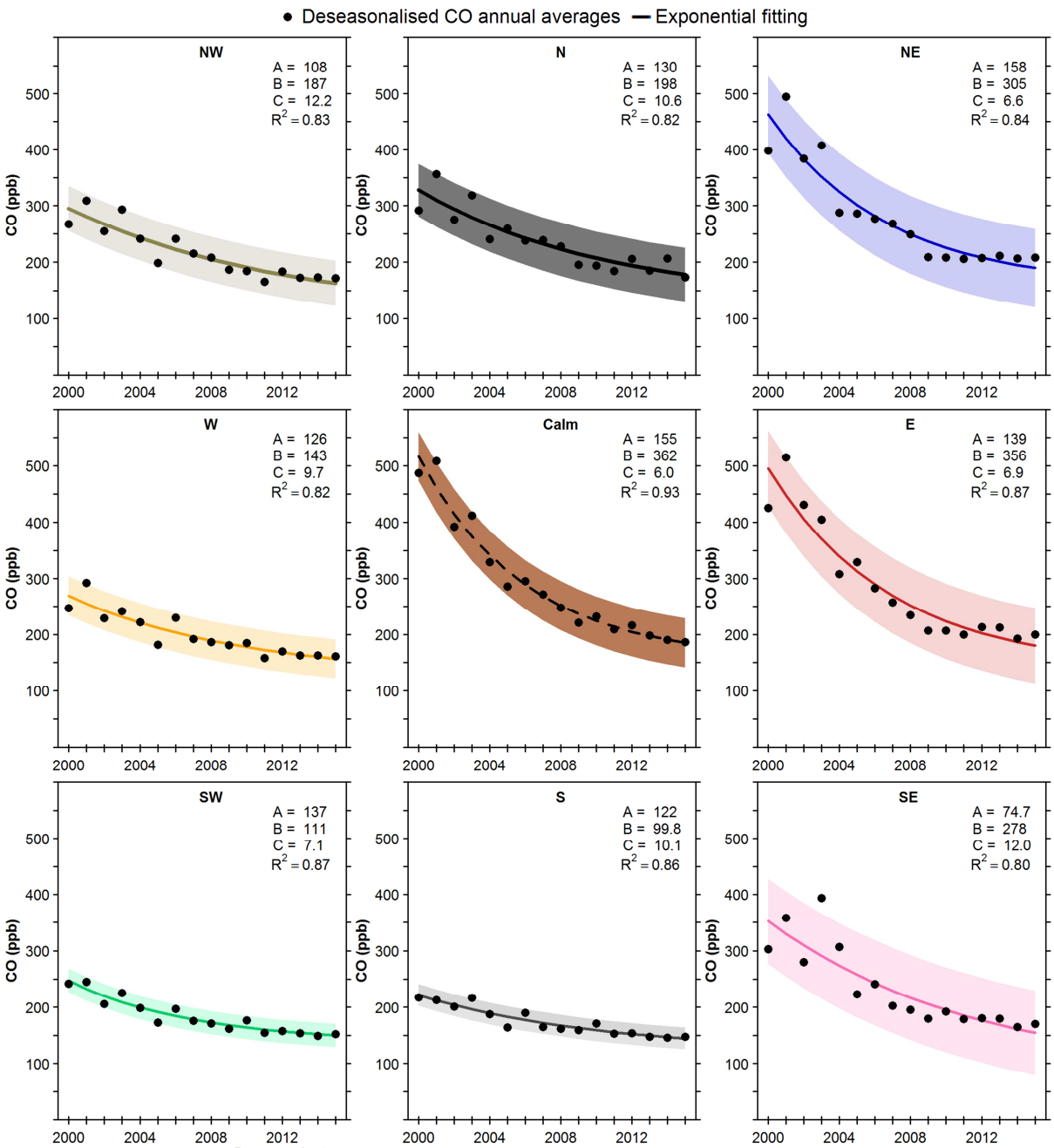

Fig. 8. Exponential decay in de-seasonalised annual averages of CO recorded at EGH by wind sector during 2000-2015. De-seasonalised annual averages were computed with the STL technique. The shading shows 95 % confidence intervals estimated through bootstrap resampling. As reported by Lowry et al. (2016), the best fit to the data are exponential curves to the de-seasonalised annual CO averages, with an offset exponential function of the form: $y = A + Be^{\frac{-(x-x_0)}{c}}$, where x_0 is the initial year of measurements, 2000. The parameters A, B and C, and the correlation coefficient for each wind sector are shown in their respective panels.

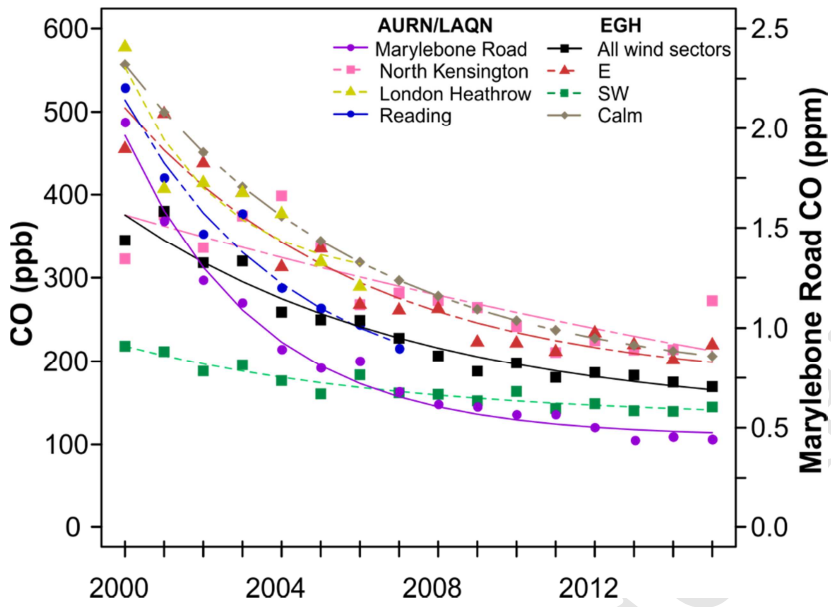

Fig. 9. Trends in CO ambient observed in SE England during 2000-2015 and comparison with changes in CO for the E, SW, calm and all wind sectors at EGH during the same period. LAQN site names LH2: Heathrow airport (closed 2011), MY1: Marylebone Road and REA: Reading (closed 2007). De-seasonalised annual averages were computed with the STL technique. The shading shows 95 % confidence intervals estimated through bootstrap resampling (Carslaw, 2015). As reported by Lowry et al. (2016), the best fit to the data are exponential curves to the de-seasonalised annual CO averages, with an offset exponential function of the form: $y = A + Be^{\frac{-(x-x_0)}{c}}$, where x_0 is the initial year of measurements, 2000.

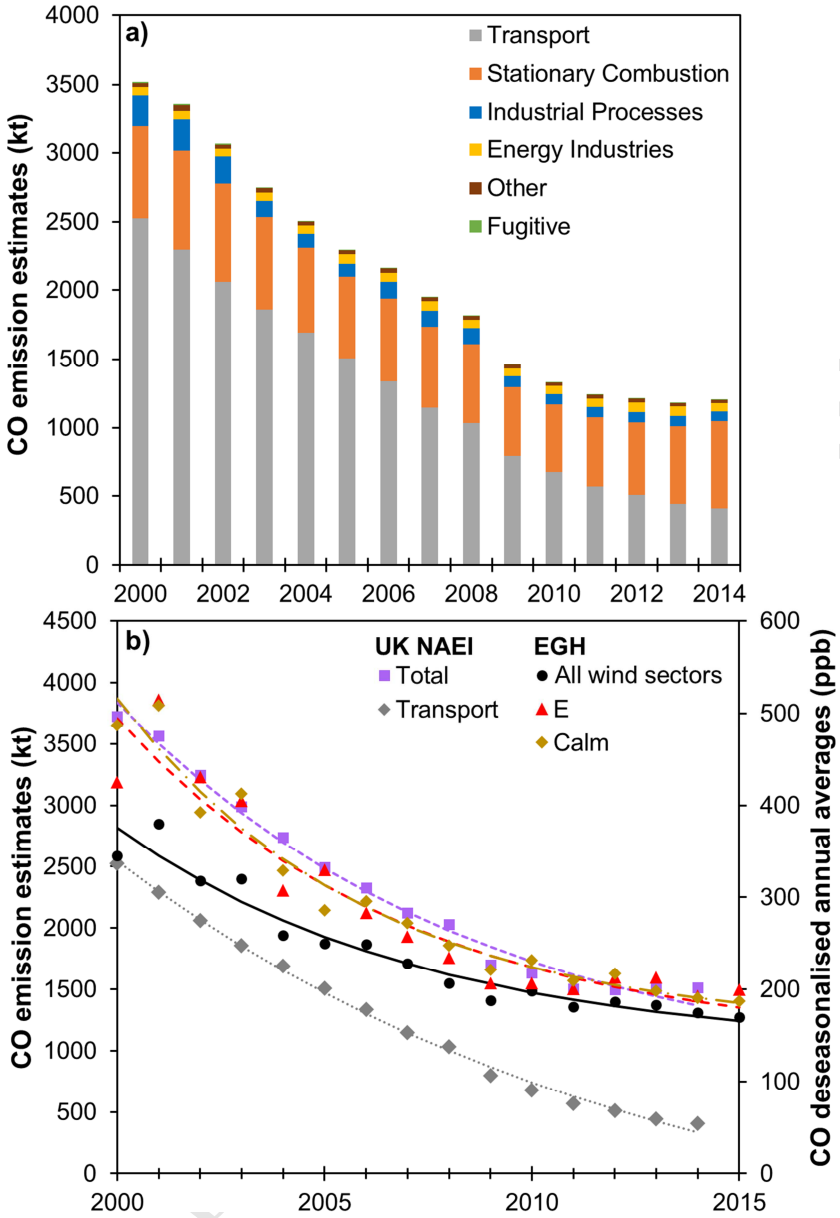

Fig. 10. (a) Trends in CO emissions during 2000-2014 in England by category as reported in the UK NAEI 2016. Stationary combustion is estimated as Industrial combustion + Residential combustion. (b) Comparison of the decay in CO estimated emissions as reported in the UK NAEI 2016 and CO measurements for all EGH wind sectors, E and calm during 2000-2015.

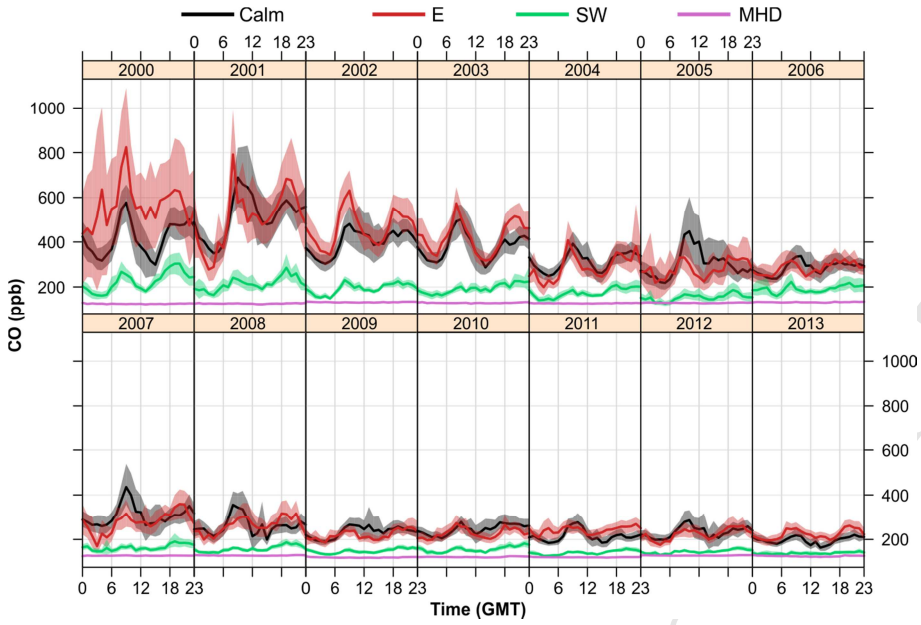

Fig. 11. CO diurnal cycles constructed from hourly averages at EGH and MHD during 2000-2013. The shading shows the estimated 95 % confidence intervals estimated through bootstrap resampling (Carslaw, 2015).

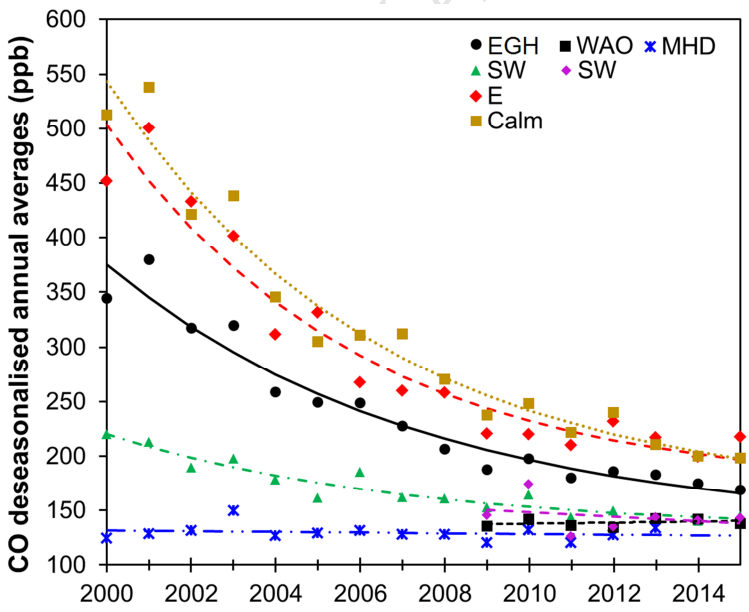

Fig. 12. Comparison between the exponential decay in CO for the E, SW, calm and all wind sectors at EGH during 2000-2015 with changes in CO at WAO for the SW and all wind sectors during 2009-2015, and MHD during 2000-2013.

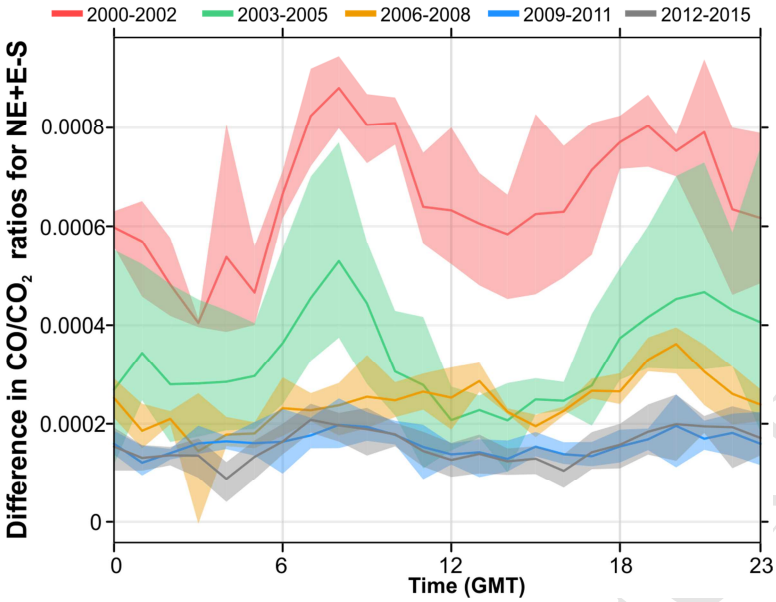

Fig. 13. Temporal analysis of the CO/CO_2 residual, i.e. the CO/CO_2 excess after subtracting S from NE-E wind sectors using a 1 h window data in the diurnal cycle. The shading shows the estimated 95 % confidence intervals estimated through bootstrap resampling (Carslaw, 2015).

Table 1. Monitoring sites description located in the Greater London Area and Reading used for CO long-term trends comparison with EGH data.

Monitoring site	QA/QC[a] standard	LAQN code	Classification	Operating period	Distance to road	Sampling height
Heathrow Airport	LAQN	LH2[b]	Industrial	1/1/1999 to 24/2/2011	N.A.	N.A.
Kensington and Chelsea – North Kensington	AURN/LAQN	KC1[c]	Urban Background	17/3/1995 to present	N.A.	3 m
Reading - New Town	AURN	RD0[c]	Urban Background	17/07/1997 to 30/09/2007	100 m	3 m
Westminster - Marylebone Road	AURN/ LAQN	MY1[c]	Kerbside	26/5/1997 to present	1.5 m	2.5 m

N.A.: Not applicable
[a]Quality Assurance and Quality Control standards
[b]Data not fully ratified for 2011
[c]Data ratified

Table 2. Statistics of CO 30-min data expressed in units of ppb recorded at EGH during 2000-2015.

Year	Average	SD	Median	Maximum
2000	343.3	109.5	238.5	3766.6
2001	386.1	141.4	265.6	3705.4
2002	318.3	99.4	236.3	2410.5
2003	324.9	92.5	243.7	2037.4
2004	255.0	79.2	199.7	2245.1
2005	254.3	97.4	183.4	2629.9
2006	239.6	59.3	199.0	2063.2
2007	228.6	82.8	180.8	1907.1
2008	208.9	64.2	171.6	1289.3
2009	185.7	48.7	161.0	1265.1
2010	197.8	55.9	173.9	1168.5
2011	178.7	52.1	151.5	1330.8
2012	186.7	42.2	159.3	1166.0
2013	183.1	51.0	153.3	1375.6
2014	175.1	45.2	150.7	988.9
2015	169.0	29.6	152.4	919.9

**Standard deviation of the annual averages calculated from monthly averages.*

Table 3. CO decline rates during 2000-2015 calculated by wind sector at EGH.

Wind sector*	N	NE	E	SE	S	SW	W	NW	Calm
ppb yr^{-1}	8.6	13.9	18.7	10.2	4.7	5.9	6.5	7.7	17.9
% yr^{-1}	2.9	3.8	4.8	3.7	2.4	2.7	2.8	3.0	4.6
Overall decline (%)	46.4	60.8	76.8	59.2	38.4	43.2	44.8	48.0	73.6

*All declines are significant at $p<0.001$.

Highlights

1. CO data recorded at Egham (EGH) in Southwest London during 2000-2015 were analysed.
2. CO varies on time scales ranging from minutes to inter-annual and annual cycles.
3. CO declined at EGH more slowly than in Central London, but from a much lower starting point.
4. The largest decline rates were observed for the calm and Eastern wind sectors.
5. Assessment of CO/CO_2 residuals confirmed a clear decline in CO during periods of increased vehicle traffic from 2000 to 2015.